Available online at www.sciencedirect.com

ScienceDirect

journal homepage: www.elsevier.com/locate/burns

Ephrin-A2 affects wound healing and scarring in a murine model of excisional injury

Dulharie Wijeratne [a], *Jennifer Rodger* [b], *Andrew Stevenson* [a], *Hilary Wallace* [a], *Cecilia M. Prêle* [c,d], *Fiona M. Wood* [a,d,e,f], *Mark W. Fear* [a,c,e,*]

[a] *Burn Injury Research Unit, School of Biomedical Sciences, The University of Western Australia, Australia*
[b] *Experimental and Regenerative Neurosciences, School of Biological Sciences, The University of Western Australia, Australia*
[c] *The Institute for Respiratory Health, The University of Western Australia, Nedlands, Western Australia, Australia*
[d] *Centre for Cell Therapy and Regenerative Medicine, School of Biomedical Sciences, The University of Western Australia, Crawley, Western Australia, Australia*
[e] *The Fiona Wood Foundation, Perth, Western Australia, Australia*
[f] *Burns Service of Western Australia, WA Department of Health, Perth, Western Australia, Australia*

ARTICLE INFO

Article history:
Accepted 4 October 2018

Keywords:
Ephrin A2
Collagen
Scarring
Wound repair
Keratinocyte

ABSTRACT

Ephrin ligand/Eph receptor signaling is important in both tissue development and homeostasis. There is increasing evidence that Ephrin/Eph signaling is important in the skin, involved in hair follicle cycling, epidermal differentiation, cutaneous innervation and skin cancer. However, there is currently limited information on the role of Ephrin/Eph signaling in cutaneous wound healing. Here we report the effects of the Ephrin-A2 and A5 ligands on wound healing. Using Ephrin-A2$^{-/-}$, Ephrin-A5$^{-/-}$ and Ephrin-A2A5$^{-/-}$ transgenic mice, *in vitro* wound healing assays were conducted using isolated keratinocytes and fibroblasts. Ephrin-A2$^{-/-}$, Ephrin-A2A5$^{-/-}$ and wild type mice with excisional wounds were used to analyze the impact of these ligands on wound closure, scar outcome, collagen orientation and re-innervation *in vivo*.

The absence of the Ephrin-A2 and A5 ligands did not have any effect on dermal fibroblast proliferation or on fibroblast or keratinocyte migration. The loss of Ephrin-A2 and A5 ligands did not impact on the rate of wound closure or re-innervation after injury. However, changes in the gross morphology of the healed scar and in collagen histology of the scar dermis were observed in transgenic mice. Therefore Ephrin-A2 and A5 ligands may play an important role in final scar appearance associated with collagen deposition and structure.

* *Corresponding author at*: Burn Injury Research Unit, M318, University of Western Australia, 35 Stirling Highway, Crawley, WA 6009 Australia.
E-mail address: Mark.fear@uwa.edu.au (M.W. Fear).
https://doi.org/10.1016/j.burns.2018.10.002

1. Introduction

Eph receptor/Ephrin ligand interactions are important in neuronal mapping and topography in central and peripheral nerves [1]. All the Eph receptors and Ephrin ligands are expressed in normal human skin [2] and Ephrin-A ligand signaling has been shown to be important in hair follicle cycling and epidermal differentiation [3–5]. Ephrin A2 and A5 are critical for sensory axonal growth patterning and in the development of cutaneous innervation in animal models [4–7]. In addition, keratinocytes treated with human Fc-conjugated Ephrin-A ligands have been shown to suppress the expression of important cell adhesion genes such as integrin β6 and integrin β4, suggesting Ephrin signaling may influence cell migration through reduced cell attachment and increased motility [4]. Eph A3 mediated activation of Ephrin A2 or A5 signaling has also been shown to result in increased cell adhesion to laminin through increased β1 integrin expression [8]. Since β1 integrin plays an important role in wound repair [9] this evidence suggests Ephrin signaling may be important in skin repair after injury. Ephrin signaling is also important in skin cancer, with significant roles in melanoma and more recently demonstrated role in squamous cell carcinoma (SCC), with a key role for ephrin signaling in migration and invasion of tumour cells [10–12]. Ephrin signaling has also been implicated in the response to hypoxia in the skin, potentially implicating ephrin signaling in angiogenesis in wound repair as well as in tumours [13]. However, whilst all this evidence points to an important role for ephrin signaling in wound repair, to date there have been no studies demonstrating the effects of ephrin signaling on scar formation after cutaneous injury *in vivo*. We hypothesized that Ephrin A2 and/or A5 signaling would be important in wound repair. Specifically, with the known role for these ligands in the development of cutaneous innervation, and the well-known changes in innervation associated with scar [14–16], we hypothesized the absence of these ligands would result in decreased innervation in scar. We also hypothesized that Ephrin A2 and/or A5 signaling may affect healing through modulation of keratinocyte migration. Here, using Ephrin A2$^{-/-}$, Ephrin A5$^{-/-}$ and Ephrin A2$^{-/-}$A5$^{-/-}$ transgenic mice and an excisional injury model, we have investigated the potential impact of Ephrin A2 and A5 on wound repair both in vitro and *in vivo*.

2. Materials and methods

2.1. Animals

C57BL/6 wild type mice, Ephrin-A2$^{-/-}$ mice, Ephrin-A5$^{-/-}$ mice and Ephrin-A2A5$^{-/-}$ mice were maintained in standard housing with food and water provided *ad libitum*. Approval was obtained by Institutional ethics committees and experiments performed in accordance with the National Health and Medical Research Council (NHMRC) Australian Code of Practice for the Care and Use of Animals for Scientific Purposes. (RA/3/100/1162).

2.2. In vitro scratch assay

Dermal fibroblasts from Wild-type (n=5), Ephrin-A2$^{-/-}$ (n=5), Ephrin-A5$^{-/-}$ (n=5) and Ephrin-A2A5$^{-/-}$ (n=5) mice were isolated, cultured and plated in 6 well tissue culture plates. The seeding density of dermal fibroblasts was 2×10^5/ml of Dulbecco's modified eagle medium nutrient mixture F-12 (DMEM/F12, GIBCO® Carlsbad, California, USA) supplemented with 10% fetal bovine serum (FBS, Invitro technologies, Noble Park North, Australia) and 1% penicillin/streptomycin (GIBCO® by Life Technologies, Carlsbad, California, USA). Plates were incubated at 37°C in 5% CO_2 for the cells to reach full confluence over two days when a scratch was made as previously described [17]. Photographs were taken at 0, 6, 24, 30 and 48 h using a light microscope (Olympus IX51, Japan) at a final objective 10×, numerical aperture 0.13. The total photographed area and the area of the scratch was measured using the ImageJ software program [18]. The percentage closure was calculated by subtracting the percentage of the scratch area remaining at each time point from the percentage of the scratch at 0 h (100%) to obtain the percentage closure (% surface area of the scratch that was covered by cells). Cell migration was represented as the percentage closure of the scratch over time.

2.3. Primary dermal fibroblast proliferation assay

Dermal fibroblasts from wild-type (n=5), Ephrin-A2$^{-/-}$ (n=5), Ephrin-A5$^{-/-}$ (n=5) and Ephrin-A2A5$^{-/-}$ (n=5) mice, were seeded at 1.5×10^3 cells per well in 96 well microplates in 100 μl of DMEM/F12 supplemented with 10% FBS and 1% penicillin/streptomycin. Each sample contained 3–5 replicate wells. Control wells contained 100 μl of DMEM/F12 supplemented with 10% FBS and 1% penicillin/streptomycin. Cells were incubated at 37°C with 5% CO_2. Separate plates were used for 24, 48, 72 and 96 h incubation times after seeding dermal fibroblasts. At each time-point, 20 μl of CellTiter 96® AQueous Non-Radioactive cell solution (Promega cooperation, Madison, USA) was added into each well including the control wells and incubated for 3 h. Absorbance was read at 492 nm using a Multiskan Transmit RC program (Labsystems, Frankland, Massachusetts, USA). The mean absorbance of all the samples in each genotype at each time point was calculated and plotted to provide a measure of proliferation/viability of each cell type over time.

2.4. Keratinocyte isolation and culture

Fur was removed from the dorsal mouse skin and cleaned with povidone-iodine solution (Pfizer, Perth pty limited) and 70% ethyl alcohol using autoclaved cotton wool. Dorsal skin was harvested using scissors. Skin was collected in 1 ml of Epigrow™ human epidermal keratinocyte complete media (Merck, Millipore, Massachusetts, USA). Skin tissue was cut into pieces of 3–5 mm^2. The pieces of skin were collected in 5 ml of Epigrow™ human epidermal keratinocyte complete media with 20 μl of fungizone (Gibco®, Invitrogen™, Carlsbad, California, USA) and 100 μl of kanamycin (Gibco®, Invitrogen™, Carlsbad, California, USA). 0.0127 g of Dispase (Life technologies™, Carlsbad, California, USA) per 5 ml (2.4U/ml) was added. This solution was incubated for 24 h at 4°C.

After 24h, the epidermis was separated from the dermis using sterile fine tip forceps and the pieces of epidermis transferred into 500μl of Tryple Select (Gibco®, Invitogen™, Carlsbad, California, USA) placed in a sterile petri dish. The epidermal tissue pieces were spread out flat on the surface of Tryple Select and to prevent evaporation of the solution the petri dish was covered with a lid. After an incubation period of 20 to 30min at room temperature the petri dish was tilted at a 30° angle and 2ml of human epidermal keratinocyte complete media was added. With the help of sterile forceps epidermal tissue pieces were rubbed gently against the base of the petri dish in order to generate a single cell suspension. The resulting cell suspension was collected in a 15ml centrifuge tube and the previous step repeated to increase the yield of keratinocytes. The combined cell preparation was then centrifuged at 200g for 3min. The cell pellet was resuspended in 5ml of human epidermal keratinocyte complete media. Cells were cultured on T25 tissue culture flasks (Sarstedt, Germany) coated with 1ml of 20μg/ml type IV collagen in phosphate buffered saline (type IV from human placenta, Sigma-Aldrich, Missouri, USA) [19].

2.5. Keratinocyte migration assay (time lapse microscopy)

A glass bottom dish with a diameter of 35mm and an inner glass diameter of 10mm (Mat Tek co-operation, Massachusetts, USA) was coated with 20μg/ml of collagen IV in PBS[19]. Keratinocytes from Wild-type (n=3), Ephrin-A2$^{-/-}$ (n=3), Ephrin-A5$^{-/-}$ (n=3) and Ephrin-A2A5$^{-/-}$ (n=3) mice were seeded at a density of 1×10^5 cells/cm^2 and incubated for 24h at 37°C with 5% CO_2 [20]. Keratinocytes were visualised at a magnification of 10× and a numerical aperture of 0.55 using differential interference contrast (DIC) and an Olympus IX81 inverted microscope (Olympus, Tokyo, Japan). Images were taken at an interval of 1min for 1h with a resolution of 1376×1032 pixels by a U-TV1X-2 camera (Olympus, Tokyo, Japan). The distance of the keratinocyte nuclear migration was measured using the Fiji software package [20].

2.6. Full thickness surgical excisional wound injury

Wild-type (n=7), Ephrin-A2$^{-/-}$ (n=7) and Ephrin-A2A5$^{-/-}$ (n=7) mice aged 8weeks were given 7days to acclimatize to animal handling and the environment. On the day of surgery, mice aged 9weeks were given general anesthesia using isofluorane administered by anesthetic chamber and maintained by facemask. While the animal was under general anesthesia the area to be wounded was shaved and cleaned with povidone-iodine solution (Pfizer, Perth pty limited). A sterile 12mm punch biopsy (Acuderm inc., Fort Lauderdale, USA) was used to create an incision on the back of the mouse. Using sterile surgical scissors the tissue was removed following the outline made by the punch biopsy incision, creating a 12mm diameter full-thickness excisional wound. The wound was created away from all limbs and on one side of the back away from the spine to prevent impacting on movement and activity. The wound was covered with tegaderm dressing using tissue adhesive to maintain the dressing in place. All animals were given buprenorphine for analgesia (0.1mg/kg intramuscular) immediately prior to surgery. Oral paracetamol in drinking water (1mg/ml) was given for 5days after injury. Once recovered the animals were group housed and allowed food and water *ad libitum*.

2.7. Imaging and sample collection

A Canon Powershot S100 digital camera was used to photograph wounds daily for the first seven days after injury and then at days 9,11,13,14 and 16. The total wound area and the scar (circularity and the size) were measured using the ImageJ image processing and analysis program as previously described [18,20].

Mice were sacrificed 28days after injury and scar tissue collected and fixed in Zamboni's fixative and tissue samples embedded in paraffin for further analysis.

2.8. Assessment of collagen density and orientation

Masson trichrome staining was carried out after excisional injury (day 28) scar tissue pieces obtained from wild type (n=5), Ephrin-A2$^{-/-}$ (n=5) and Ephrin-A2A5$^{-/-}$ (n=5) mice. Three sections were used from each animal. Stained sections were imaged at 10x magnification through stereology software using a Nikon Eclipse 90i upright microscope (Nikon Corporation, Tokyo, Japan).

Density and orientation of collagen was assessed using image J software [18]. Collagen stained by Masson's Trichrome was measured using FIJI using the color threshold and analyze tool. Collagen density was measured by restricting the "hue" threshold to the green region of the spectrum. Once only the green was selected, the "select" tool was used in the color threshold window and the "analyse>measure" function was then used to count pixels. The hue threshold was then opened back up to include all colors and the whole tissue selected, by adjusting the brightness down to exclude the white background. This was then selected and measure the same way. The area covered by the green collagen was then divided by the area of total tissue to give a measure of percentage collagen per tissue. Orientation of collagen was assessed using previously described protocol [21].

2.9. Assessment of cutaneous re-innervation

Epidermal and dermal nerve density of wild type (n=6), Ephrin-A2$^{-/-}$ (n=6) and Ephrin-A2A5$^{-/-}$ (n=6) mice were detected using protein gene product (PGP) 9.5 (Abd Serotec Oxford, UK) immunohistochemistry as previously described [6] Three tissue sections and one field from a tissue section were used to quantify epidermal and dermal nerve density per animal. Imaging and quantification was carried out as previously described [6].

2.10. Statistical analyses

All results were analysed using SPSS version 19. Non-parametric Kruskal-Wallis test ($p=0.05$) was used in all analyses. Individual comparisons were made between each Ephrin-A$^{-/-}$ and wild type mice using the Mann-Whitney U test ($p=0.05$).

3. Results

3.1. *Ephrin-A2 & -A5 ligands have no significant effect on dermal fibroblast proliferation or fibroblast and keratinocyte migration in vitro*

The proliferation rate of wild type, Ephrin-A2$^{-/-}$, Ephrin-A5$^{-/-}$ and Ephrin-A2A5$^{-/-}$ dermal fibroblasts was assessed using the MTS colorimetric assay. There was no significant difference in the average proliferation rate of dermal fibroblasts between 24 to 96h after incubation (Kruskal Wallis; $p > 0.05$) between the four genotypes (Fig. 1a). Using a scratch closure assay, all scratch injuries were completely closed by fibroblasts after 96h in all four genotypes (Fig. 1b). There was no statistically significant difference in the percentage closure of the scratch injury at any time point (Kruskal Wallis; $p > 0.05$). Therefore the absence of either the Ephrin-A2 or A5 ligands does not appear to affect dermal fibroblast proliferation or migration *in vitro*.

The migration rate of wild type, Ephrin-A2$^{-/-}$, Ephrin-A5$^{-/-}$, and Ephrin-A2A5$^{-/-}$ keratinocytes was assessed using time lapse imaging (Fig. 1c). There was no significant difference in the keratinocyte migration rate among the four genotypes (Kruskal Wallis; $p > 0.05$). However, a trend for reduced migration was observed with keratinocytes from the Ephrin-A2k/o mice and therefore an effect on migration cannot be ruled out (Fig. 1c).

3.2. *Ephrin-A2 & -A5 ligands have no effect on the rate of excisional wound closure in vivo*

Excisional wound closure of wild type (Fig. 2a–c), Ephrin-A2$^{-/-}$ (Fig. 2d–f) and Ephrin-A2A5$^{-/-}$ (Fig. 2g–i) was measured to identify whether Ephrin-A2 and/or Ephrin-A5 ligands have an effect on the rate of wound closure. Wound closure, which is defined as a stable covering [26] was completed by day 16 after injury in all four genotypes (Fig. 2j). There was no significant difference in the rate of wound closure among the three genotypes at any time point (Kruskal Wallis; $p > 0.05$).

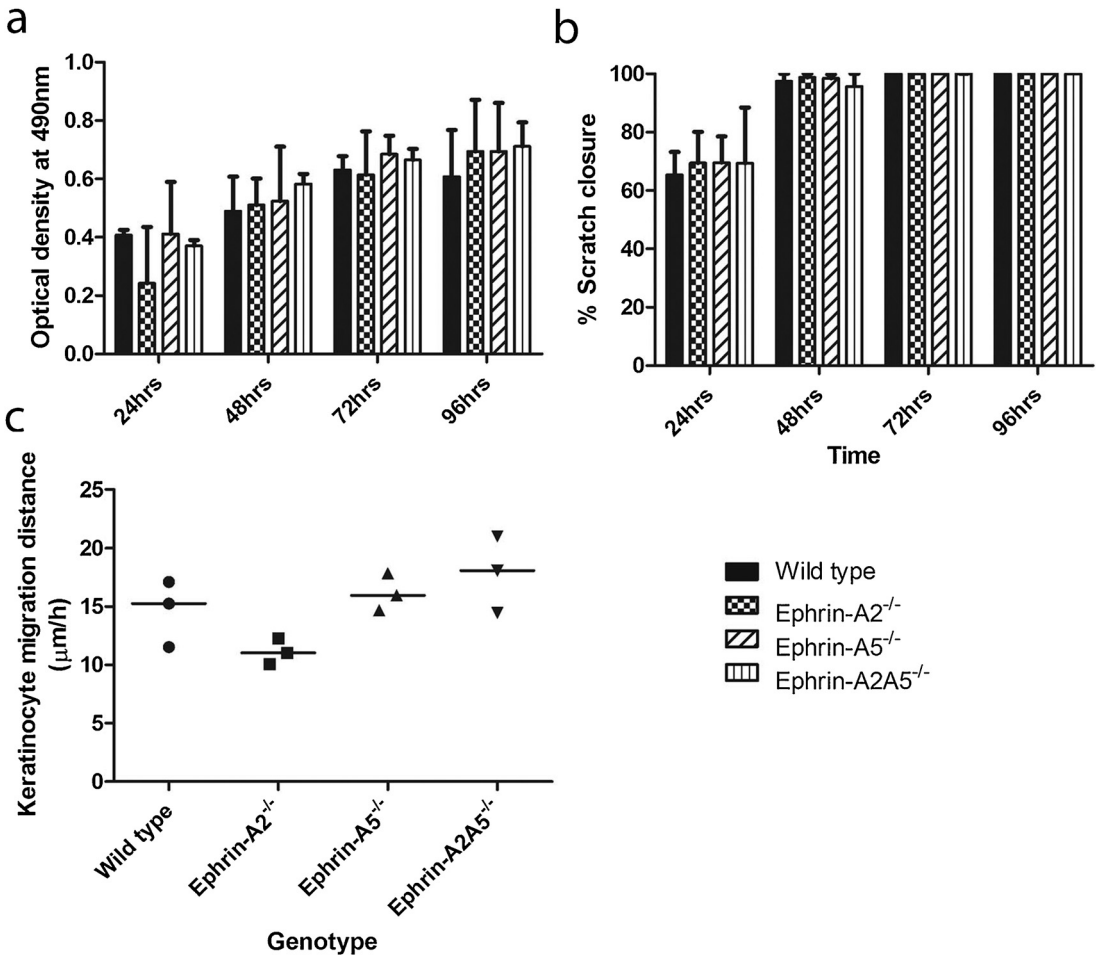

Fig. 1 – Proliferation and migration of fibroblasts and keratinocytes isolated from wild type, Ephrin-A2$^{-/-}$, Ephrin-A5$^{-/-}$ and Ephrin-A2$^{-/-}$A5$^{-/-}$ genotype mice is unchanged.
(a) Proliferation (MTS) assay over 96h for fibroblasts from wild type, Ephrin-A2$^{-/-}$, Ephrin-A5$^{-/-}$ and Ephrin-A2$^{-/-}$A5$^{-/-}$ genotypes.
(b) Rate of closure of scratch (migration assay) for fibroblasts from wild type, Ephrin-A2$^{-/-}$, Ephrin-A5$^{-/-}$ and Ephrin-A2$^{-/-}$A5$^{-/-}$ genotypes.
(c) Direct migration measurements for keratinocytes from wild type, Ephrin-A2$^{-/-}$, Ephrin-A5$^{-/-}$ and Ephrin-A2$^{-/-}$A5$^{-/-}$ genotypes. $^{*}p \leq 0.05$

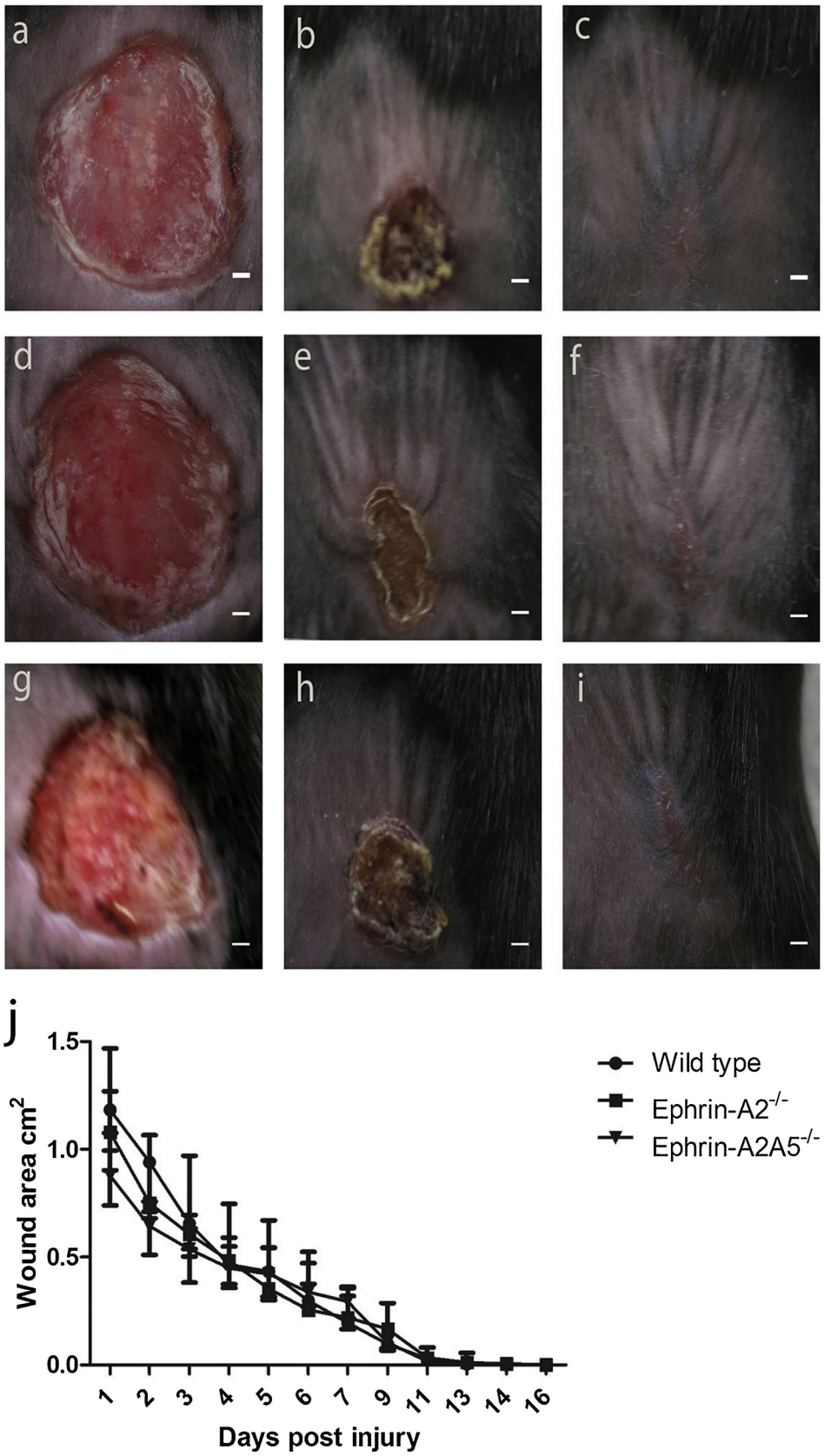

Fig. 2 – Wound closure rate of an excisional injury is not affected in Ephrin-A2$^{-/-}$ and Ephrin-A2$^{-/-}$A5$^{-/-}$ genotype mice. (a–c) Excisional wound closure of wild type mice, day 1, day 7 and day 16 after injury (a–c respectively). (d–f) Excisional wound closure of Ephrin-A2$^{-/-}$ mice. Day 1, day 7 and day 16 after injury (d–f respectively). (g–i) Excisional wound closure of Ephrin-A2$^{-/-}$A5$^{-/-}$ mice. Day 1, day 7 and day 16 after injury (g–i respectively).

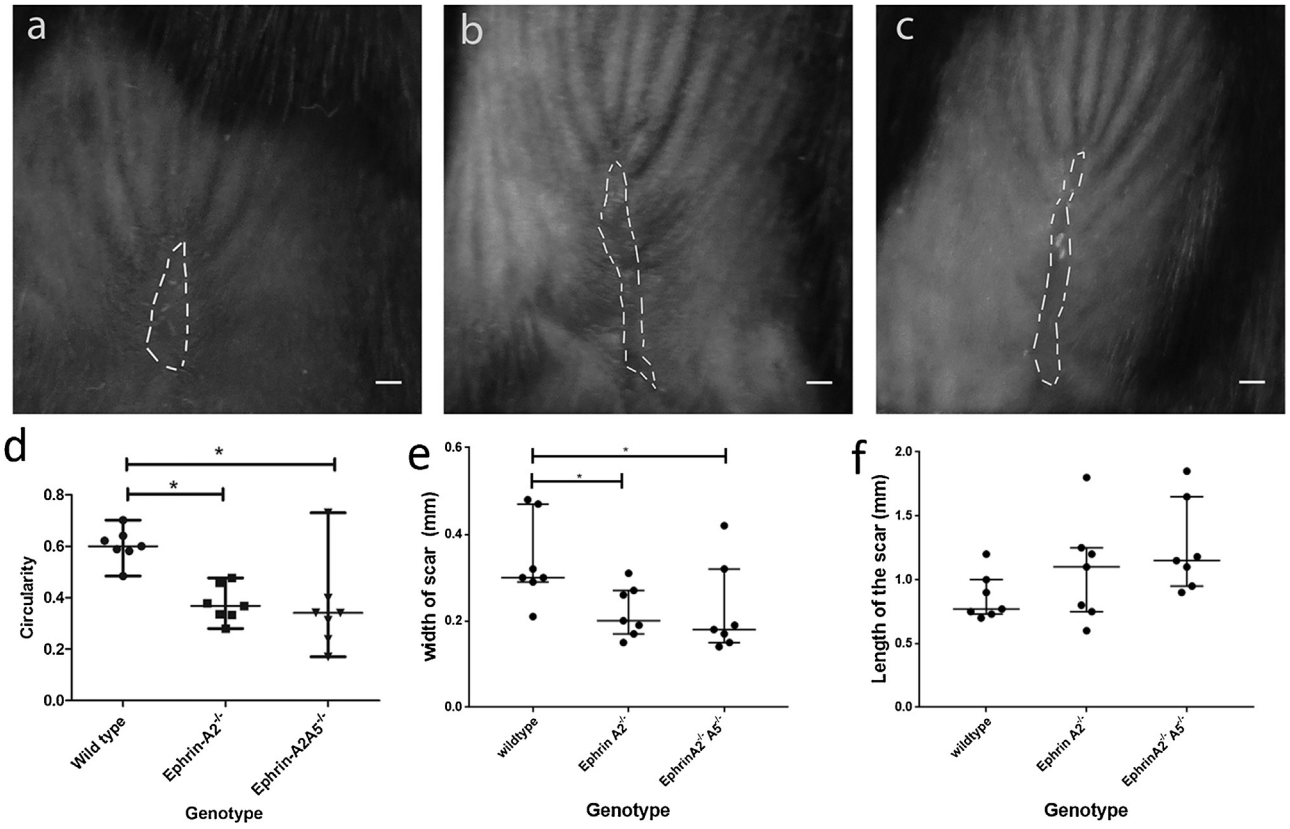

Fig. 3 – Scar morphology is altered in in Ephrin-A2$^{-/-}$ and Ephrin-A2$^{-/-}$A5$^{-/-}$ genotype mice.
(a–c) Wound scar outcome of wild type (a), Ephrin-A2$^{-/-}$ (b) and Ephrin-A2$^{-/-}$A5$^{-/-}$ (c) at 16 days after injury. Scale bar: 1 mm. (d–f) Circularity of the scars and width and length of measured scars (d–f respectively). n=7 Animals per genotype. Data are represented as median and IQR. *p < 0.05.

3.3. *Ephrin-A2 & -A5 ligands have an effect on wound contracture and gross morphology*

Wound healing and contracture of injuries in wild type mice occurs in all directions leading to a circular scar similar in shape to the original injury but significantly reduced in size (primarily due to contraction of the wound). In Ephrin-A2$^{-/-}$ and Ephrin-A2A5$^{-/-}$ mice healing appeared to be impacted as the resulting scar (observed at day 16 after injury), although of similar surface area (Kruskal Wallis; $p > 0.05$), was observed to be more linear compared to wild type mice with a longer, but more narrow scar in the anterior/posterior direction (Fig. 3a–f). The circularity of the scars was significantly reduced in both Ephrin-A2$^{-/-}$ and Ephrin-A2A5$^{-/-}$ mice compared to wildtype controls (Kruskal Wallis; $p < 0.05$, (Fig. 3d)). Scar width was significantly reduced in both Ephrin-A2$^{-/-}$ and Ephrin-A2A5$^{-/-}$ mice compared to wildtype controls (Kruskal Wallis; $p < 0.05$, (Fig. 3e)). Scar length was not significantly different but there was a trend for increased length in the Ephrin-A2$^{-/-}$ and Ephrin-A2A5$^{-/-}$ mice compared to wildtype controls (Fig. 3f).

3.4. *Ephrin-A2 & -A5 ligands have an effect on scar collagen deposition in vivo*

Using Masson's trichrome staining the collagen deposition in scars of the mice at day 28 after injury were assessed (Fig. 4a–c). Density of Collagen in the dermis was significantly increased in A2$^{-/-}$ mice compared to control wildtype mice and Ephrin A2$^{-/-}$A5$^{-/-}$ mice ($p = 0.016$, Fig. 4d). Coherency of Collagen showed a trend to be increased (more striated and aligned) in A2$^{-/-}$ mice compared to control and A2$^{-/-}$A5$^{-/-}$ mice but this was not significant (Fig. 4e).

3.5. *Ephrin-A2 & -A5 ligands do not have any effect on epidermal and dermal re-innervation in vivo*

Epidermal and dermal re-innervation was not significantly different between the three genotypes in the scar tissue biopsies (Fig. 5a–e (Kruskal Wallis; $p > 0.05$)).

n=7 animals per genotype. Data are represented as median and IQR. Scale bar: 0.1 mm.
(j) Rate of wound closure in mice is not significantly different between genotypes.

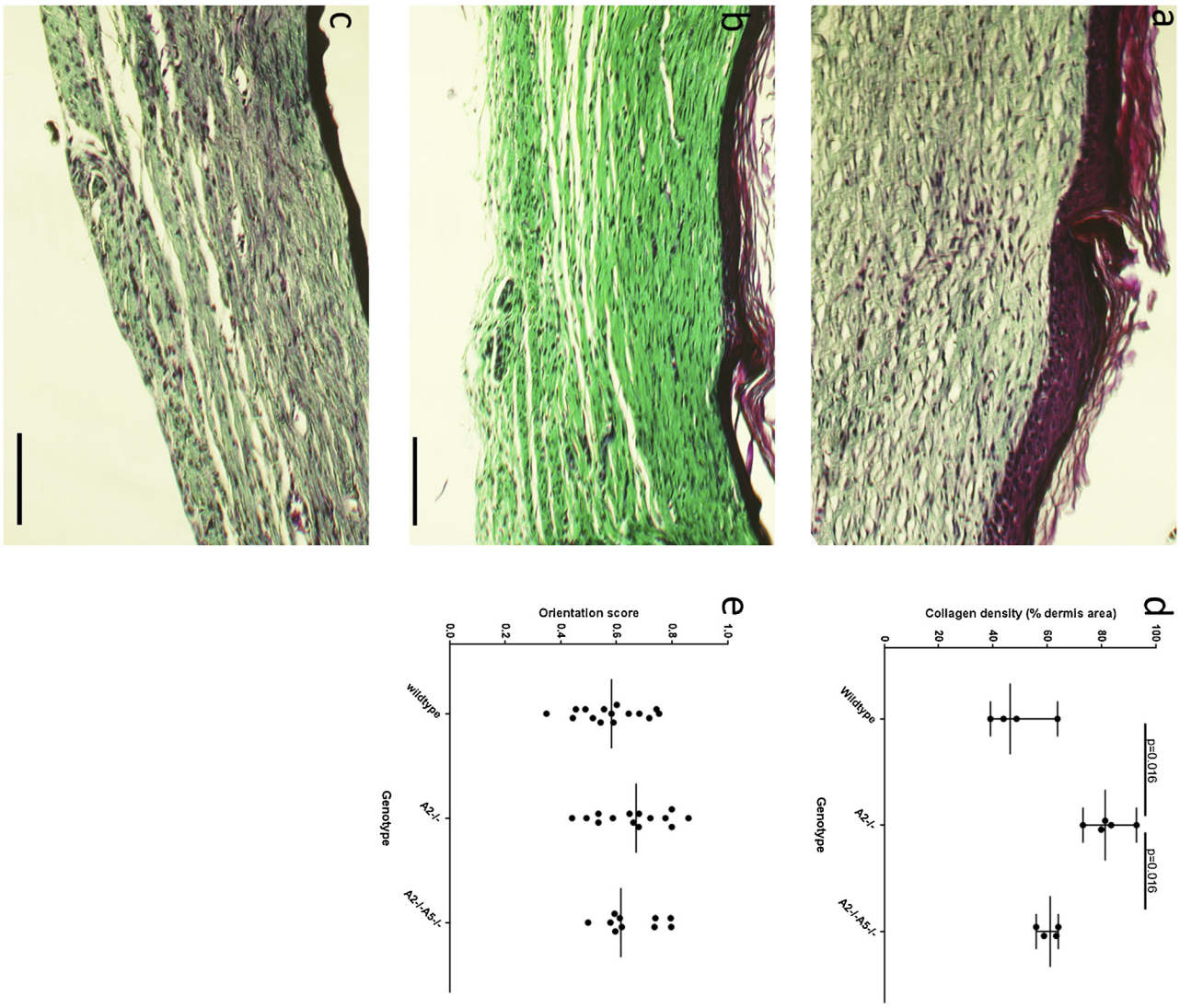

Fig. 4 – Collagen deposition in scar tissue is altered in Ephrin A2$^{-/-}$ and Ephrin A2$^{-/-}$A5$^{-/-}$ mice.
(a–c) Masson trichrome staining of scars at day 28 after injury for wildtype, Ephrin-A2$^{-/-}$ and Ephrin-A2$^{-/-}$A5$^{-/-}$ mice (a–c respectively).
(d) Density of collagen in the scars at 28 days after injury in Ephrin-A$^{-/-}$ and wild type mice. Ephrin-A2$^{-/-}$ show significantly increased collagen density compared to wild type mice and A2$^{-/-}$A5$^{-/-}$ mice.
(e) Collagen orientation score in scars at 28 days after injury. n = 5 animals per genotype. Data are represented as median and IQR.

4. Discussion

The current study showed no significant effect of the absence of either the Ephrin A2 or Ephrin A5 ligand on dermal fibroblast migration or proliferation and keratinocyte migration *in vitro*. *In vivo* wound healing analysis shows that these two ligands do not appear to affect the rate of wound closure. Both ligands appear to have effects on scar outcome, potentially through an impact on contraction of the wound and collagen orientation. However Ephrin A2 and A5 ligands did not appear to have any impact on cutaneous re-innervation during wound healing.

Dermal fibroblasts from Ephrin A2$^{-/-}$, A5$^{-/-}$ and A2$^{-/-}$A5$^{-/-}$ mice showed a normal rate of proliferation *in vitro* when compared to wild type cells. By contrast, stimulation of endogenous EphA with Ephrin A1 inhibited the proliferation of several cell types via negative regulation of the Ras/MAPK pathway [22]. However the data presented here suggest neither Ephrin A2 nor Ephrin A5 ligands are critical to fibroblast proliferation.

Previous studies have shown an impact of Ephrin B/EphB signaling on melanoblast and neural crest cell migration [23] Other studies have demonstrated an importance for ephrin signaling in the migratory phenotype of other cells [4,24] and changes in integrin expression in keratinocytes after Ephrin signaling modulation suggests that Ephrin signaling could play a role in the control of cell migration after injury [4,8]. However,

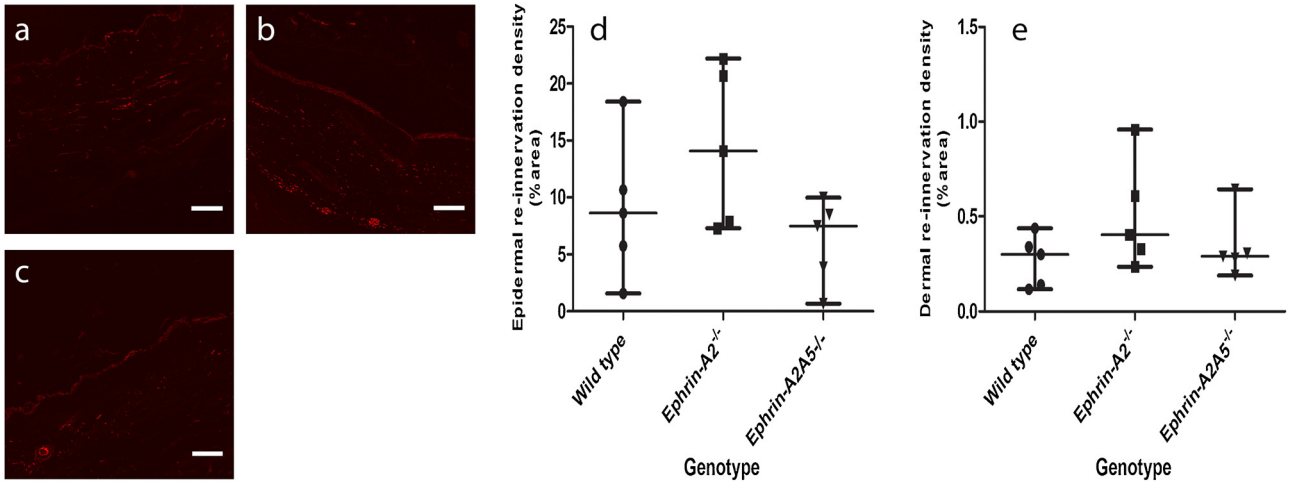

Fig. 5 – Reinnervation after excisional injury in Ephrin wild type, Ephrin-A2$^{-/-}$ and Ephrin-A2$^{-/-}$A5$^{-/-}$ genotype mice.
(a-c) Representative images of PGP9.5 immunohistochemistry in scar tissue from wild type, Ephrin A2 $^{-/-}$ and Ephrin A2$^{-/-}$A5 $^{-/-}$ mice after excisional injury.
(d-e) Quantitation of epidermal and dermal innervation using PGP9.5 immunohistochemistry in scar tissue from all 3 genotypes. Data are represented as median and IQR. $^{*}p < 0.05$

in this study no significant effect of the absence of the Ephrin A2 or Ephrin A5 ligand on either keratinocyte or fibroblast migration was observed. This may reflect redundancy of Ephrin signaling, with other family members compensating for the absence of these Ephrins. However, no effect was observed in these assays even with the A2$^{-/-}$A5$^{-/-}$ double knockout cells, suggesting a lack of effect of the Ephrins in this model rather than compensation. The lack of an effect may also be related to the use of a single cell type. The nature of Ephrin signaling requires bi-directional interactions between receptor and ligand expressing cells. This may occur *in vivo* between different cell types during healing but the effect is lost when testing using a single cell type. It is important to note that the data obtained for keratinocyte migration contained fewer samples than that for the fibroblast data, due to technical issues with isolation and maintenance of the keratinocytes from these mice. Therefore the lack of effect observed in this study may in the case of keratinocytes simply reflect the limited sample number being insufficient to detect a difference. This is suggested by the trend toward altered migration observed and the findings of others. Nevertheless, no change in the rate of wound closure was observed in the transgenic mice. This strongly suggests that the loss of Ephrin A2 and A5 do not negatively impact on re-epithelialisation. This may be surprising in light of other studies indicating a role for Ephrin signaling in cell migration, and as discussed may reflect redundancy or that Ephrins other than A2 and A5 are important for keratinocyte migration and wound closure.

Surprisingly, whilst there appears to be no effect of Ephrin-A2 or A5 on wound closure rates, a marked difference in the gross morphology of scars in transgenic mice was observed. This was also reflected in a change in the dermal matrix, with the collagen matrix significantly denser compared to controls and with a trend to increased fibre alignment in scars of A2$^{-/-}$ transgenic animals. Previously, Ephrin-A1 has been shown to induce expression of a number of extracellular protein genes, including increasing expression of fibrillar collagen [4]. *In vivo*, it appears that the loss of Ephrin A2/A5 ligands leads to increased collagen deposition with a more aligned architecture of the dermal matrix as seen in poor scars. This suggests that ephrin signaling may be involved in fibroblast communication during healing and impact on the resultant matrix deposition. The changes to the matrix and in particular to the gross morphology of the scars suggest there may be a relationship between tension, healing and ephrin expression. In particular the change to the scar shape may indicate a change in contracture and response to tension. This requires further investigation.

Previously we reported that Ephrin-A2 and -A5 ligands play an important role in the development of cutaneous nerves [5] and we consequently expected changes in cutaneous innervation to be observed in the scar tissue. However no differences were observed. This suggests these ligands are not important in cutaneous re-innervation after excisional wounding. This could be due to differential Eph/Ephrin expression patterns during the wound healing process or functional redundancy of the Ephrin molecules. However functional testing was not conducted after the injury due to difficulty in obtaining accurate information from the very small scar area, and the use of PGP9.5 staining, whilst providing a useful indicator of overall innervation, does not provide a complete picture. In addition, as with the keratinocyte migration data, there were limited tissue samples available for this part of the study. This limits the power to detect changes, especially in light of the significant variation between samples. Therefore it is possible that there are effects of Ephrin A2 and A5 on reinnervation that have not been observed in this study.

This is the first time Ephrin expression has been implicated *in vivo* in scar formation. In particular the effect on collagen deposition and the matrix architecture are of significant interest given the potential to modulate matrix deposition

through Ephrin signaling. This interesting result requires further investigation to understand the mechanism by which these Ephrins impact on scar formation as well as their normal physiological role. This could ultimately lead to novel ways of intervention in wound repair to ameliorate scar formation and improve patient outcomes.

5. Conflict of interest

The authors state no conflict of interest.

Acknowledgments

The authors acknowledge the facilities, and the scientific and technical assistance of the Australian Microscopy & Microanalysis Research Facility at the Centre for Microscopy, Characterisation & Analysis, The University of Western Australia, a facility funded by the University, State and Commonwealth Governments. MF is supported by Chevron Australia.

REFERENCES

[1] Palmer A, Klein R. Multiple roles of ephrins in morphogenesis, neuronal networking, and brain function. Genes Dev 2003;17:1429–50.
[2] Hafner C, Becker B, Landthaler M, Vogt T. Expression profile of Eph receptors and ephrin ligands in human skin and downregulation of EphA1 in nonmelanoma skin cancer. Mod Pathol 2006;19:1369–77.
[3] Yamada Y, Midorikawa T, Oura H, Yoshino T, Ohdera M, Kubo Y, et al. Ephrin-A3 not only increases the density of hair follicles but also accelerates anagen development in neonatal mice. J Dermatol Sci 2008;52:178–85.
[4] Walsh R, Blumenberg M. Specific and shared targets of ephrin A signaling in epidermal keratinocytes. J Biol Chem 2011;286:9419–28.
[5] Lin S, Gordon K, Kaplan N, Getsios S. Ligand targeting of EphA2 enhances keratinocyte adhesion and differentiation via desmoglein 1. Mol Biol Cell 2010;21:3902–14.
[6] Wijeratne DT, Rodger J, Wallace HJ, Maghami S, Sykes M, Wood FM, et al. Ephrin-A2 and Ephrin-A5 are important for the functional development of cutaneous innervation in a mouse model. J Invest Dermatol 2015;135:632–5.
[7] Munoz LM, Zyachkivsky A, Kunz RB, Hunt JM, Wang G, Scott SA. Ephrin-A5 inhibits growth of embryonic sensory neurons. Dev Biol 2005;283:397–408.
[8] Huai J, Drescher U. An ephrin-A-dependent signaling pathway controls integrin function and is linked to the tyrosine phosphorylation of a 120-kDa protein. J Biol Chem 2001;276:6689–94.
[9] Grose R, Hutter C, Bloch W, Thorey I, Watt FM, Fassler R, et al. Crucial role of beta 1 integrins for keratinocyte migration in vitro and during cutaneous wound repair. Development 2002;129:2303–15.
[10] Farshchian M, Nissinen L, Siljamaki E, Riihila P, Toriseva M, Kivisaari A, et al. EphB2 promotes progression of cutaneous squamous cell carcinoma. J Invest Dermatol 2015;135:1882–92.
[11] Lin S, Wang B, Getsios S. Eph/ephrin signaling in epidermal differentiation and disease. Semin Cell Dev Biol 2012;23:92–101.
[12] Hendrix MJ, Seftor EA, Hess AR, Seftor RE. Molecular plasticity of human melanoma cells. Oncogene 2003;22(20):3070–5.
[13] Song Y, Zhao XP, Song K, Zheng-Jun S. Ephrin-A1 is up-regulated by hypoxia in cancer cells and promotes angiogenesis of HUVECs through a coordinated cross-talk with eNOS. PLoS One 2013;8(9):e74464.
[14] Reynolds ML, Fitzgerald M. Long-term sensory hyperinnervation following neonatal skin wounds. J Comp Neurol 1995;358:487–98.
[15] Zhang LQ, Laato M. Innervation of normal and hypertrophic human scars and experimental wounds in the rat. Ann Chir Gynaecol 2001;90(215):29–32.
[16] Whitby DJ, Ferguson MW. The extracellular matrix of lip wounds in fetal, neonatal and adult mice. Development 1991;112:651–68.
[17] Morellini NM, Giles NL, Rea S, Adcroft KA, Falder S, King CE, et al. Exogenous metallothionein-IIA promotes accelerated healing after a burn wound. Wound Repair Regen 2008;16:682–90.
[18] Schneider CA, Rasband WS, Eliceiri KW. NIH Image to ImageJ: 25 years of image analysis. Nat Methods 2012;9:671–5.
[19] Redvers RP, Kaur P. Serial cultivation of primary adult murine keratinocytes. Methods Mol Biol 2005;289:15–22.
[20] Schindelin J, A.Rganda-Carreras I, Frise E, Kaynig V, Longair M, Pietzsch T, et al. Fiji: an open-source platform for biological-image analysis. Nat Methods 2012;9:676–82.
[21] Clemons TD, Bradshaw M, Toshniwal P, Chaudhari N, Stevenson A, Lynch J, et al. Coherency image analysis to quantify collagen architecture: implications in scar assessment. RSC Adv 2018;8:9661–9.
[22] Miao H, Wei BR, Peehl DM, Li Q, Alexandrou T, Schelling JR, et al. Activation of EphA receptor tyrosine kinase inhibits the Ras/MAPK pathway. Nat Cell Biol 2001;3:527–30.
[23] Santiago A, Erikson CA. Ephrin-B ligands play a dual role in the control of neural crest cell migration. Development 2002;129:3621–32.
[24] Yamazaki T, Masuda J, Omori T, Usui R, Akiyama H, Maru Y. EphA1 interacts with integrin-linked kinase and regulates cell morphology and motility. J Cell Sci 2009;122:243–5.